ISSN 8756-6990, Optoelectronics, Instrumentation and Data Processing, 2017, Vol. 53, No. 5, pp. 421–430. © Allerton Press, Inc., 2017.
Original Russian Text © A.I. Antonov, G.I. Greisukh, E.G. Ezhov, S.A. Stepanov, 2017, published in Avtometriya, 2017, Vol. 53, No. 5, pp. 4–16.

DIFFRACTIVE OPTICS

Diffractive Elements for Imaging Optical Systems

A. I. Antonov, G. I. Greisukh*, E. G. Ezhov, and S. A. Stepanov**

Penza State University of Architecture and Construction,
ul. Germama Titova 28, Penza, 440028 Russia
**E-mail: grey@pguas.ru*
***E-mail: subscribing_2002@mail.ru*

Received May 15, 2017

Abstract—The problems and prospects of using diffractive elements with a sawtooth relief-phase microstructure in imaging optical systems are analyzed. Particular attention is paid to minimizing the adverse side effect of diffraction orders on the quality of the image formed by an optical system with a diffractive element due to the change-over from single-layer microstructures to structures containing several layers and reliefs. Requirements are formulated for the design parameters of the microstructure and operating conditions of diffractive elements in optical systems that ensure no visible halo caused by adverse diffraction orders. It is shown by a number of examples that the use of a diffractive element in a plastic-lens imaging optical system corrects chromatic aberrations and provides high resolution in the generated image.

Keywords: diffractive optical element, sawtooth relief-phase microstructure, imaging optical system, diffraction efficiency, optical image quality.

DOI: 10.3103/S8756699017050016

INTRODUCTION

The main purpose of including diffractive optical elements (DOEs) in imaging optical systems is to correct aberrations, primarily chromaticity. In particular, a DOE with a concentric annular microstructure [1] of small optical power provides high chromaticity correction required to obtain high-quality color images, even when using a limited range of optical materials, e.g. commercially available optical plastics [2]. The change-over from optical glass to plastics allows high-volume fabrication of lenses with aspherical refractive surfaces and diffractive microrelief on an spherical or a spherical surface [3]. This significantly improves the opportunity of correcting monochromatic aberrations and ultimately ensures the production of competitive compact high-resolution optical systems for photo and video cameras of mobile devices, video recorders, etc.

However, in addition to the positive effect, the diffractive mechanism of wavefront conversion by the diffractive lens microstructure creates a number of problems associated with the negative effect of the spurious light diffracted into side orders. Indeed, using the well-known formula of diffraction efficiency derived in scalar diffraction theory [4, 5], it is easy to show that in the case of a diffractive lense with a sawtooth relief-phase microstructure, which provides diffraction efficiency close to 100 % at a visible wavelength ($0.4 \leqslant \lambda \leqslant 0.7$ μm), the efficiency at the ends of the range decreases to 75 %. In this case, 25% of the light power falls on side diffraction orders, and the ratio of their diffraction efficiencies depends on the wavelength [6, 7]. This phenomenon, called the spectral dependence of the diffraction efficiency, plays a very negative role: in particular, it is responsible for the occurrence of a color halo around the brightest parts of the image formed by the optical system in polychromatic light. Experimental studies have shown that the probability of the formation of a halo can be reliably evaluated from the reduction in diffraction efficiency in the working diffraction order [8].

A solution to the problem of decreasing the spectral dependence of the diffraction efficiency of a transmissive microstructure and equalizing with some accuracy the efficiency in the working order in a predetermined

spectral range is proposed in [9, 10]. This solution involves constructing a two-layer relief-phase microstructure in a plane-parallel plate of two optical materials, each of which is bounded by a flat and a relief surface. The relief surfaces are similar, have the same depth, and are in optical contact with each other. Similar solutions have also been proposed by other authors (e.g., [11]).

An essential condition for reducing the spectral dependence of the diffraction efficiency of a two-layer and actually one-layer microstructure is a certain ratio between the refractive indices and dispersion ratios of the layer materials (material with higher refractive index should have a high dispersion ratio — Abbe's number [12]). In the case of optical glasses, the most appropriate pair of materials is heavy crown and light flint. Unfortunately, today, there are no pairs of technological and commercially available optical plastics with the required ratio of optical constants. Nevertheless, a solution has been proposed [13] aimed at reducing the spectral dependence of the diffraction efficiency of relief-phase microstructures made of such materials. A positive effect is achieved through the use of two reliefs of different depths.

Diffraction efficiency depends on the incident light wavelength, the angle of light incidence on the microstructure, the form and depth of the relief, and the number of Fresnel zones in the microstructure of the diffractive lens. In this case, by a Fresnel zone is meant the microstructure portion within which the phase delay introduced into the wavefront incident on it varies from 0 to 2π [14]. For a relatively large number of Fresnel zones (more than 100), high diffraction efficiency is provided by a linear sawtooth relief. For a small number of Fresnel zones, the optimal relief form depends on the form of the incident wavefront, the optical power of the diffractive lens, and the shape of the surface to which the diffractive lens microstructure is applied. In [15, 16], reliefs of optimal form that provide both maximum diffraction efficiency and the designed form of the resulting wavefront are called correlated or matched. The same papers present equations for correlated reliefs of one-layer and two-layer double-relief microstructures placed on flat and curved interfaces. It is shown that in the case of two-layer double-relief microstructures with correlated reliefs for angles of light incidence on the microstructure not exceeding 15–17°, the diffraction efficiency across the entire visible spectral range may not fall below 95 % regardless of the number of Fresnel zones in the diffractive microstructure.

Thus, when designing a DOE and selecting the type of microstructure of the element, it is necessary to take into account and reduce the negative impact of the above factors even at the cost of complication of the microstructure design and hence the fabrication of the element.

This paper provides an overview of developments in the field of DOE applications in imaging optical systems.

DESIGNS, CALCULATION, AND INVESTIGATION OF MULTILAYER MICROSTRUCTURES

Most of the recent interest in this area (with rare exceptions, see, e.g., papers [17–19] dealing with three-layer microstructures) has focused on two-layer microstructures, primarily due to the relative simplicity of their design. As noted in the introduction and shown in Fig. 1, such microstructures can contain one [9] or two reliefs [20].

For a chosen multilayer microstructure design, the calculation of its parameters reduces to the optimal choice of optical layer materials and relief depths. The optimization result obviously depends on the choice of the estimator. We are aware of at least three approaches to choosing the estimator. In the first approach,

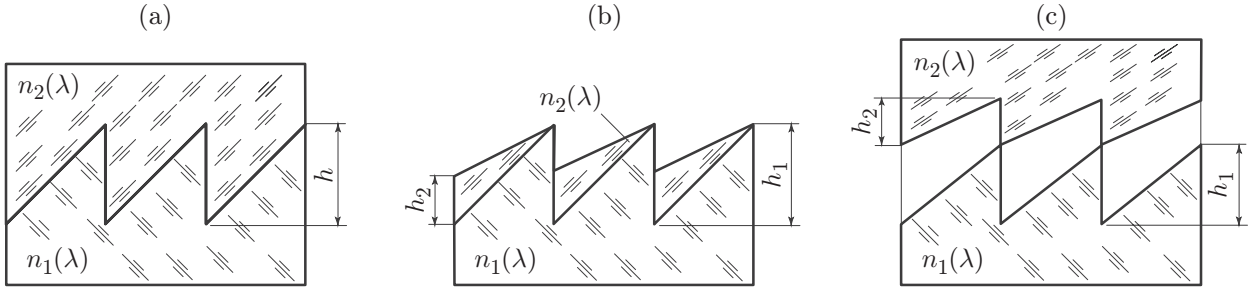

Fig. 1. Two-layer sawtooth relief-phase microstructures with a weak spectral dependence of the diffraction efficiency: (a) with one internal relief, (b) with internal and external reliefs, (c) with two internal reliefs.

the multi-layer microstructure parameters (for the chosen materials, these are the depths of the reliefs) are calculated assuming that the diffraction efficiency of the microstructure reaches its maximum at several wavelengths of the predetermined spectral range, whose number is equal to the number of the microstructure layers [11]. The depths of the reliefs are determined by solving the corresponding system of equations. Analysis of the compatibility of the equations is performed to formulate requirements for the refractive indices and dispersion characteristics of the optical materials of the multilayer microstructure. Similar approach has been used in a number of papers devoted to the calculation of two-layer microstructures with a reduced spectral dependence of the diffraction efficiency [21, 22]. From a computational point of view, this approach is the simplest and allows analytical solution based on scalar diffraction theory.

To take into account the contribution to the light diffraction efficiency from all wavelengths of the selected spectral range in the optimization of two-layer microstructure parameters with a reduced spectral dependence of the diffraction efficiency, it has been proposed [23] to use as an estimator the integrated polychromatic diffraction efficiency

$$\eta(\lambda_{\min}, \lambda_{\max}) = \int_{\lambda_{\min}}^{\lambda_{\max}} \eta(\lambda)\, d\lambda.$$

This estimator, in our opinion, is the most suitable in the case where a DOE is used to focus polychromatic light into a spot of predetermined size, like, e.g., a solar concentrator. However, in imaging optical systems, a dip in the diffraction efficiency at any working wavelength can lead to a halo without significantly affecting the polychromatic diffraction efficiency. In optimization of the microstructure parameters, this fact can be taken into account by estimating the minimum diffraction efficiency within the predetermined spectral range and the range of angles of light incidence on the microstructure [13]. This value is calculated, as a rule, in the scalar diffraction approximation. In this approximation, the dependence (on both the light wavelength λ and the angle of light incidence on the microstructure θ) of the diffraction efficiency in any diffraction order of microstructures having an arbitrary number of reliefs and layers can be estimated by the formula [5]

$$\eta_m = \Big[\frac{\sin\left(\pi(m - \Delta l/\lambda)\right)}{\pi(m - \Delta l/\lambda)}\Big]^2,$$

where m is the diffraction order number, Δl is the increment of the optical path in one period (one annular zone) of the sawtooth profile, which depends on the angle of light incidence on the microstructure θ, the refractive indices of the materials $n_i(\lambda)$, and the relief depths h_i.

In the case of a two-layer single-relief microstructure (Fig. 1a), the optical path increment is given by [24]

$$\Delta l = h\Big(\sqrt{n_1^2 - \sin^2\theta} - \sqrt{n_2^2 - \sin^2\theta}\Big),$$

and in the case of two-layer microstructures with internal and external reliefs or with two internal reliefs, shown in Figs. 1b and 1c, the value of Δl is calculated by the formula [18]

$$\Delta l = h_1\Big(\sqrt{n_1^2 - \sin^2\theta} - \cos\theta\Big) - h_2\Big(\sqrt{n_2^2 - \sin^2\theta} - \cos\theta\Big).$$

The applicability of scalar diffraction theory to the calculation of the diffraction efficiency of both single-layer and multilayer microstructures devoted to the analysis has been analyzed in a large number of papers. In particular, it has been shown [25] that the diffraction efficiency of two-layer microstructures obtained using rigorous diffraction theory based on the solution of the Maxwell equations with appropriate boundary conditions is generally lower than that predicted by scalar theory. However, if the relative minimum period of the microstructure satisfies the condition $\Lambda_{\min}/h \geqslant 10$, where h is the total depth of the relief, this difference between the diffraction efficiencies is insignificant and can be neglected. The above condition is generally used to calculate microstructures included in imaging optical systems. For the cases where this condition is not satisfied, a simplified geometrical method for estimating the diffraction efficiency of multilayer microstructures has been proposed [26], which, in our opinion, gives fairly accurate estimates of the angular dependence of the diffraction efficiency.

Nevertheless, scalar diffraction theory remains the main tool not only for calculating (especially at a preliminary stage) but also for studying multilayer microstructures. For example, this approximation has been

used [27] to estimate the effect of manufacturing errors of a two-layer double-relief microstructure with two internal reliefs on the diffraction efficiency and to estimate [28] the effect of the temperature change of this microstructure.

IMAGING OPTICAL SYSTEMS WITH DOEs

The results of studies of the spectral and angular dependences of the diffraction efficiency of relief-phase microstructures given in [25, 29–31] have shown that when calculating imaging refractive-diffractive optical systems, it is necessary to take into account the conditions affecting the probability of halo occurrence in the image generated by such systems. In particular, these results suggest that a visible halo will be absent if the minimum relative period of the two-layer microstructure $\Lambda_{\min}/h > 10$, the angles of light incidence on the microstructure $\theta \leqslant 15{-}17^\circ$, and the diffraction efficiency of the microstructure calculated in the scalar diffraction approximation, $\eta > 0.95$ in the whole working spectral range. The above lower-bound constraints on the minimum period and diffraction efficiency of the microstructure and the upper-bound constraints on the angles of light incidence on the microstructure should be included in the procedure of layout planning, calculation, and optimization of refractive-diffractive optical systems.

To date, a number of papers (see, e.g. [17, 20, 32–34]) have been published describing imaging optical systems with multilayer DOEs. However, information about what and how effective measures were made by the authors to eliminate the negative effect of side diffraction orders on the image quality taken is either insufficient or completely absent in these publications. Therefore, in [31, 35, 36], examples are given of the most characteristic three types of refractive-diffractive optical systems for mobile cameras that meet the above requirements providing the absence of the visible halo associated with side diffraction orders.

As a first example we consider a compact eight-lens refractive-diffractive apochromatic objective [31] whose optical layout is shown in Fig. 2.

The focal length of the objective $f' = 3.7$ mm, the dimension (distance from vertex tangent plane of the front lens to the plane of the image) $L = 10.5$ mm, and all refractive surfaces of the objective lenses are aspherical. All the refractive lenses of this objective, except for the lens with the diffractive microstructure applied to one of it surfaces, are made of technological and commercially available plastics of two types: polymethylmethacrylate and polycarbonate. As for the refractive lens with the diffractive microstructure, the choice of its material depends on the working spectral range of the lens and the design and materials of the layers of this microstructure.

The best of the currently commercially available pair of materials is M-LAC14/AL-6263-(OKR4NT), which has an extended spectral range, including visible and near infrared light ($0.4 \leqslant \lambda \leqslant 0.9$ μm) and technologically the simplest two-layer one-relief microstructure [31]. The first of these materials (M-LAC14) is optical glass used to fabricate lenses by precision casting or stamping, and the second material (AL-6263-(OKR4NT)) is optical plastic. In this case, M-LAC14 glass is also the material of the refractive lens with the diffractive microstructure.

The selected pair of materials of the microstructure layers at a relief depth $h = 10.25$ μm and the maximum angle of light incidence on the microstructure $\theta_{\max} = 15^\circ$ provides a diffraction efficiency of 0.91 in the specified working spectral range. The degree of aberration correction of this objective is such that in the spectral range $0.4 \leqslant \lambda \leqslant 0.9$ μm and within the angular field $2\omega \leqslant 30^\circ$, the polychromatic diffraction frequency-contrast characteristic is not less than 0.5 at spatial frequencies of up to 100 lines/mm and is not

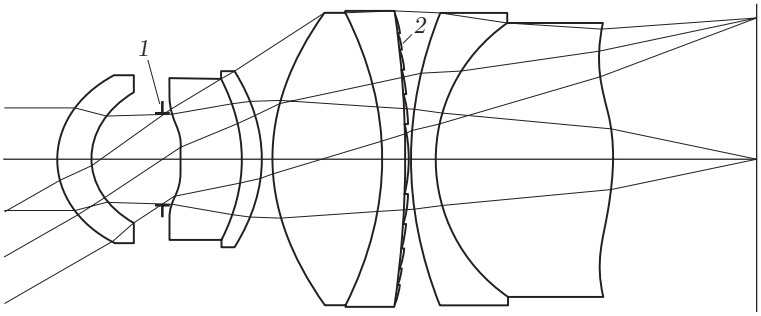

Fig. 2. Schematic of an eight-lens refractive-diffractive apochromatic objective: (*1*) aperture, (*2*) diffractive lens.

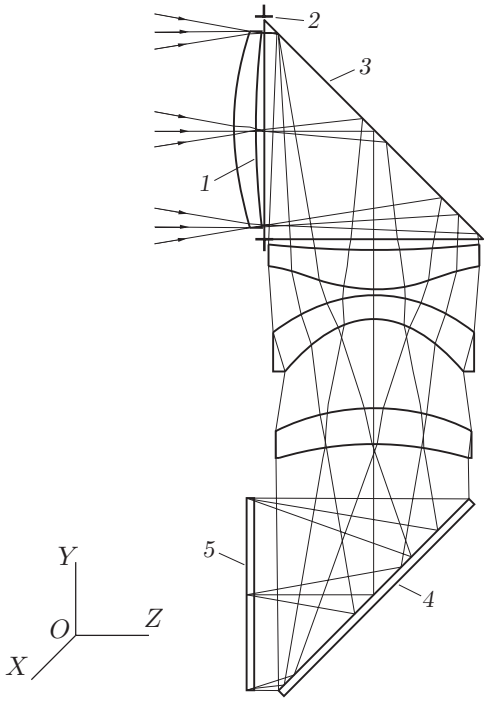

Fig. 3. Layout of the refractive-diffractive periscope-type objective: (*1*) diffractive lens, (*2*) aperture, (*3*) rotating prism, (*4*) rotating mirror, and (*5*) protective glass of the image sensor.

less than 0.2 at spatial frequencies of up to 200 lines/mm. In this case, the distortion is less than ±1 %. The minimum period of the microstructure of the diffractive lens of the objective $\Lambda_{\min} > 280$ μm ($\Lambda_{\min}/h > 25$), and the maximum angle of ray incidence on the microstructure of $\theta_{\max} \leqslant 14.3°$. And finally, if the spectral range is narrowed to $\lambda_F \leqslant \lambda \leqslant 0.8$ μm ($\lambda_F = 0.486\,13$ μm is the wavelength of the F-line in the spectrum of atomic hydrogen), the minimum diffraction efficiency rises to 0.95.

As a second example we consider an objective with a relatively large focal length, which can be embedded in a mobile communication device. Two basic requirements are imposed on the dimension of this kind of objectives. First, the objective should not occupy a lot of space inside the device. This requirement is usually formulated as follows: the volume of the parallelepiped $V = a \times b \times c$ in which the objective can be inscribed should be minimal. Second, the placement of the objective in the device should not lead to its thickening or, in other words, the size of the parallelepiped a affecting the thickness of the mobile device should correspond to its selected thickness.

In the case of a short-focal length objective, the second requirement reduces to the condition $L < a$. For long-focal length objectives, the second requirement is fulfilled, as a rule, by bending its optical axis [37]. Here the size of the parallelepiped influencing the thickness of the mobile device is determined by the effective diameter of the objective elements and, primarily by the size of the photosensitive matrix used in the device. An additional requirement to the optical layout of the objective is that the plane of the image be parallel to the smartphone motherboard, which leads to the need for a second bend of the optical axis of the objective.

The optical layout of the long-focus refractive-diffractive periscope-type objective is shown in Fig. 3. For compactness, the objective has a P–N configuration consisting of a positive (P-positive) and a negative (N-negative) lens group [35]. The positive lens group comprises a front component in the form of a refractive lens with the diffractive lens microstructure applied to one of its surfaces, a rotating prism, and a positive refractive lens. The negative lens group including two end refractive lenses comprises a negative power lens and a positive corrective lens. Except for the front lens, all positive refractive lenses are made of E48R crown-type plastic, and the material of the optically strong negative refractive lens is polycarbonate. Each surface of the plastic refractive lenses of the objective is aspherical.

The focal length of the objective $f' = 14$ mm, the focal number $K = 2.8$, the CCD format is $1/3''$ (radius of the useful image field $y' = 3$ mm), and the angular field in the object space $2\omega = 22.75°$. The objective is inscribed in a parallelepiped $6.8 \times 6.3 \times 17.4$ mm, and its side $a = 6.8$ mm is the distance between two

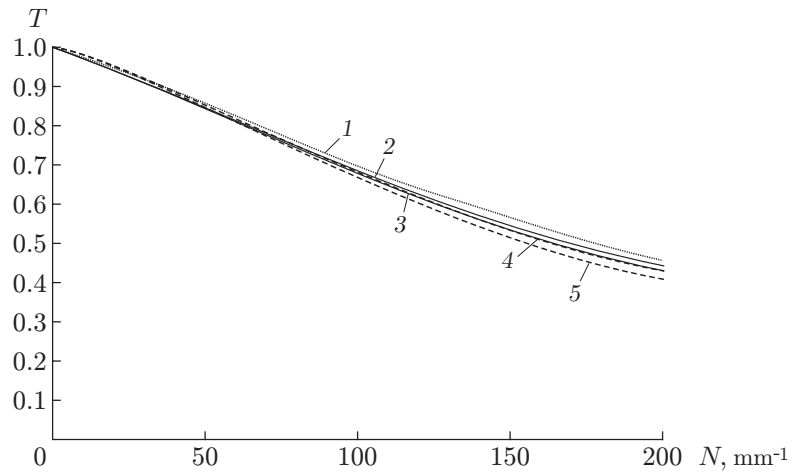

Fig. 4. Polychromatic diffraction frequency-contrast characteristic (in the meridional and sagittal planes) for the points in the image plane with the coordinates: $y' = x' = 0$ (*1*); $y' = 2.4$ mm, $x' = 1.8$ mm (*2, 3*); $y' = -2.4$ mm, $x' = 0$ (*4, 5*) (the orientation of the axes is shown in Fig. 3).

planes perpendicular to the OZ axis (see Fig. 3) and passing through the top of the front surface of the first lens and the right edge of the rotating prism.

If the working spectral range of the objective includes only visible light ($0.4 \leqslant \lambda \leqslant 0.7$ μm), then, as in the previous example, a diffractive lens with a sawtooth two-layer and one-relief microstructure made of M-NBF1 and AL-6265-(OCD-850) materials is used. Accordingly, the front lens of the objective is made of M-NBF1 glass. With the optimal relief depth $h = 6.52$ μm and the minimum relative period of the two-layer microstructure $\Lambda_{\min}/h = 14$, the diffraction efficiency will not decrease below 0.95 throughout the visible spectral range $\pm 12^\circ$ in the range of angles of light incidence on the glass or plastic microstructure (the range of angles corresponds to the above angular field of the objective $2\omega = 22.75^\circ$). This will not only ensure the absence of a halo effect, but will also eliminate any material adverse effect of diffraction orders on the quality of the image formed by the objective. Figure 4 presents the polychromatic diffraction frequency-contrast characteristic, which shows that the contrast $T > 0.4$ at spatial frequencies $N \leqslant 200$ mm^{-1} throughout the image field.

We consider a refractive-diffractive variable-focal-length objective — an optical system providing a continuous change in the scale of the image formed by it [36]. The scale change is accompanied by zooming, i. e., a change in the focal length due to smooth movement of its components. Distinctive benefits of the variable-focal-length objective lens are its simple design and compactness, i. e., the relatively small dimension ($L = 25.17$ mm) in all the configurations; a wide operating spectral range ($\lambda_F \leqslant \lambda \leqslant 0.9$ μm), including not only visible but also near infrared light, which allows the objective to be used in security surveillance devices; the material of all the lenses of the objective are commercially available optical plastics. These benefits are provided, in particular, by the optimal combination of the dispersion properties of the optical plastics and the diffractive lens, resulting in acceptable correction of primary chromaticity in all configurations of the objective that ensured the desired gradient of its focal length.

The described refractive-diffractive variable-focal-length objective with the N–P–P configuration consists of three lens groups (Fig. 5). The first (front) lens group consists of three refractive lenses; the second group consists of an aperture diaphragm, four refractive lenses, and a diffractive lens whose microstructure is applied to the back surface of the first refractive lens. Finally, the third lens group comprises a single refractive lens.

During zooming, the first lens group is fixed with respect to the photodetector and the second and third lens groups are movable. The focal length and the aperture value of the variable-focal-length objective in the short-focal, intermediate, and long-focal configurations are $f'_1 = 3.41$ mm and $K_1 = 2.99$, $f'_2 = 5.18$ mm and $K_2 = 3.97$, and $f'_3 = 8.19$ mm and $K_3 = 5.27$, respectively. A plane-parallel glass plate serving as the protective glass of the photodetector array is placed in front of the image plane. The positive refractive lenses are made of a crown-like plastic (cyclic olefin copolymer) and the negative refractive lenses are made of a flint-like polycarbonate plastic.

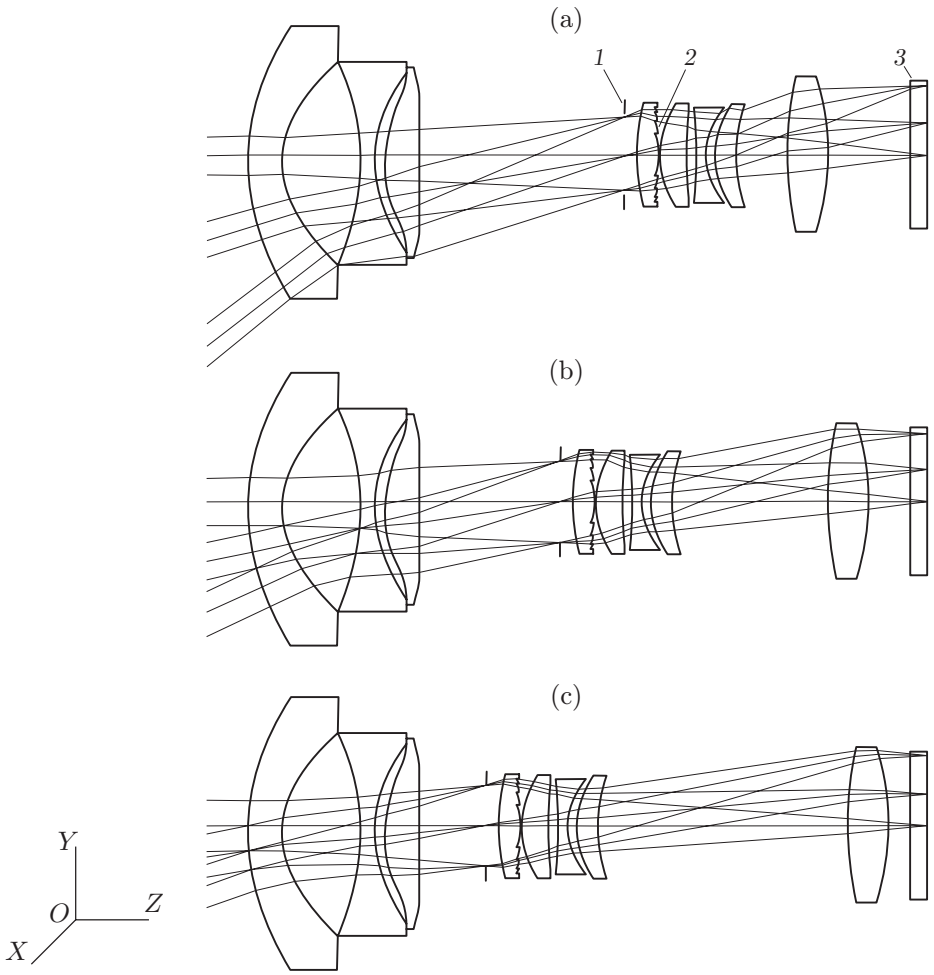

Fig. 5. Optical layout of a compact plastic-lens refractive-diffractive variable-focal-length objective: (a) short-focal-length (wide-angle) configuration $f_1' = 3.41$ mm; (b) intermediate configuration $f_2' = 5.18$ mm; (c) long-focal-length (telescopic configuration) $f_3' = 8.19$ mm. Notation: (*1*) aperture, (*2*) diffractive lens, (*3*) plane-parallel glass plate.

To reduce the spectral dependence of the diffraction efficiency, the diffractive lens microstructure should be two-layer with internal and external reliefs: the inner layer (and the refractive lens whose back surface has a microstructure) are made of cyclic olefin copolymer and the outer layer is made of polycarbonate. Optimization of the relief depths conducted for spectral range $\lambda_F \leqslant \lambda \leqslant 0.9$ mm gave the following values for the depths: $h_1^{(\mathrm{opt})} = 21.34$ μm for cyclic olefin copolymer and $h_2^{(\mathrm{opt})} = 18.36$ μm for polycarbonate. The design and parameters of the objective are such that even for its wide-angle configuration, the maximum incidence angle of the rays on the microstructure of the diffractive lens $\theta_{\max} \leqslant 16^\circ$, and the minimum period of the microstructure $\Lambda_{\min} \cong 215$ μm ($\Lambda_{\min}/h_1^{(\mathrm{opt})} > 10$). As a result, the diffraction efficiency over the entire working spectral and angular ranges is not lower than 0.92. As for the quality of the image formed by the compact plastic-lens refractive-diffractive variable-focal-length objective, it is clearly demonstrated by the curves shown in Fig. 6: the image contrast at spatial frequencies of up to 175 lines/mm is not lower than about 0.2 in any of the configurations.

CONCLUSIONS

The opportunities and challenges of using DOE in imaging optical systems were analyzed. It is shown that the main problem associated with these elements is that the quality of the formed image is adversely affected by the spurious light diffracted on the DOE microstructure into side orders. The problem is due to

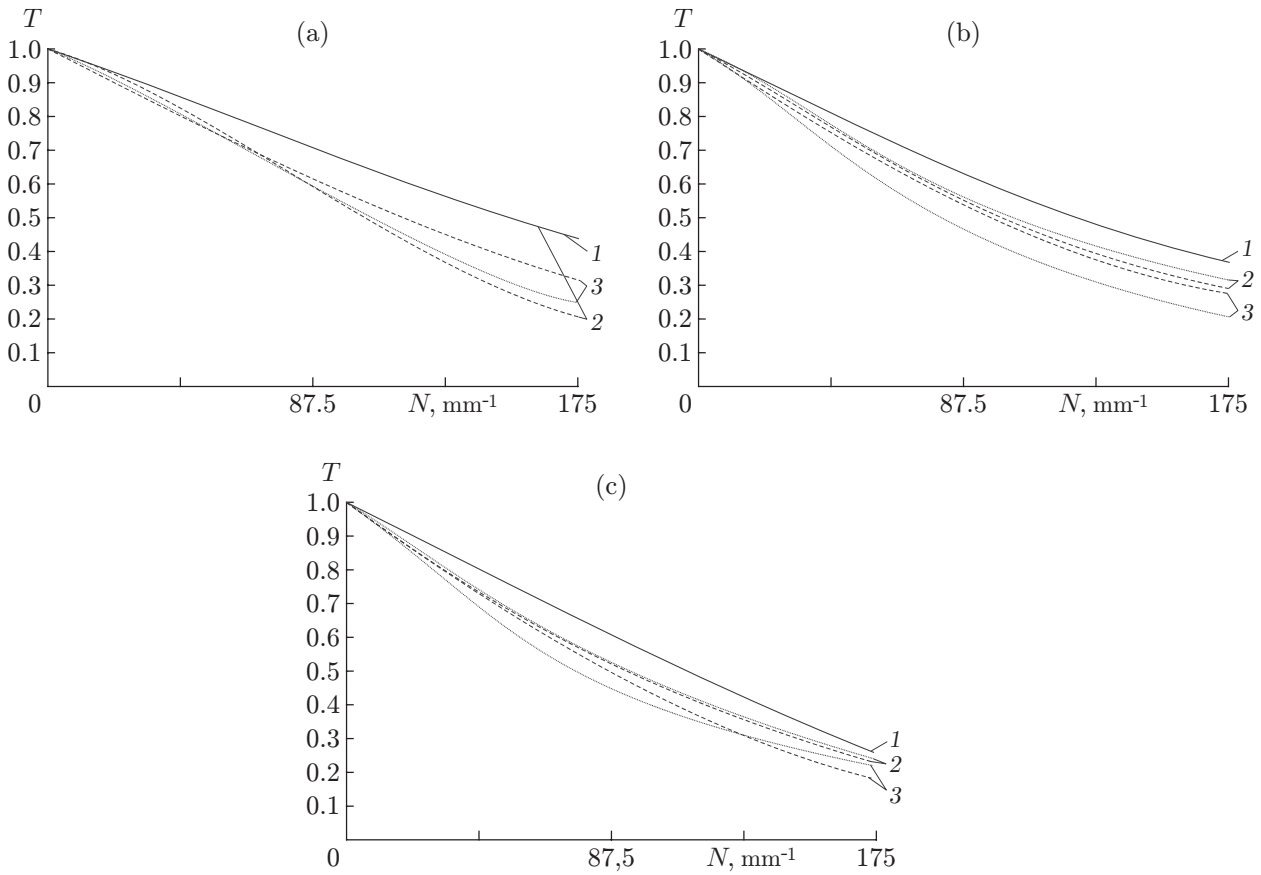

Fig. 6. Polychromatic diffraction contrast-frequency characteristic (for the meridional and sagittal planes) of a compact plastic-lens refractive-diffractive variable-focal-length objective: for the wide-angle (a), intermediate (b), and telescopic configurations (c) (calculated at the points of the image plane with the coordinates $y' = x' = 0$ (*1*); $y' = 1.25$ mm, $x' = 0$ (*2*); $y' = 2.5$ mm, and $x' = 0$ (*3*) (the orientation of the axes is shown in Fig. 5).

the spectral and angular dependences of the diffraction efficiency of the DOE. The dependence can be reduced to an acceptable level by replacing single-layer microstructures by structures comprising several layers made of materials with different optical characteristics. In particular, for two-layer single-relief microstructures, the required reduction is obtained if the layer with the higher refractive index has the higher dispersion ratio. Currently, this is achieved if at least one layer of two-layer microstructures is made of optical glass.

The change-over from single-relief to double-relief microstructures makes it possible to overcome this limitation and thereby expand the range of optical materials that can be used in multilayer microstructures, including commercially available and technological optical plastics such as polymethylmethacrylate, polycarbonate, and cyclic olefin copolymer.

It is shown that the spectral and angular dependences of the diffraction efficiency of a two-layer microstructure will be reduced to a level at which the visible deterioration of the resulting image due to side diffraction orders will be eliminated if the minimum period of the microstructure normalized to its depth $\Lambda_{\min}/h > 10$, the angles of light incidence on the microstructure $\theta \leqslant 15{-}17^\circ$, and the diffraction efficiency calculated in the scalar diffraction approximation $\eta > 0.95$ in the whole working spectral range.

Examples were given of refractive-diffractive imaging optical systems for cameras of mobile devices that meet the above requirements ensuring the absence of a visible halo due to side diffraction orders. It is shown that the inclusion of DOEs in the optical layout of plastic-lens systems corrects chromatic aberrations and provides high resolution in the resulting image.

REFERENCES

1. R. V. Shimanskii, A. G. Poleshchuk, V. P. Korol'kov, and V. V. Cherkashin, "Alignment of the Writing Beam with the Diffractive Structure Rotation Axis in Synthesis of Diffractive Optical Elements in a Polar Coordinate System," Avtometriya **53** (2), 30–38 (2017) [Optoelectron., Instrum. Data Process. **53** (2), 123–130 (2017)].
2. G. I. Greisukh, E. G. Ezhov, I. A. Levin, and S. A. Stepanov, "Design of Achromatic and Apochromatic Plastic Micro-Objectives," Appl. Opt. **49** (23), 4379–4384 (2010).
3. *Edmund Optics: Plastic Hybrid Aspheric Lenses.* https://www.edmundoptics.eu/optics/optical-lenses/achromatic-lenses/plastic-hybrid-aspheric-lenses.
4. S. T. Bobrov, G. I. Greisukh, and Yu. G. Turkevich, *Optics of Diffractive Elements and Systems* (Mashinostroenie, Leningrad, 1986) [in Russian].
5. D. A. Buralli, G. M. Morris, and J. R. Rogers, "Optical Performance of Holographic Kinoforms," Appl. Opt. **28** (5), 976–983 (1989).
6. G. I. Greisukh, E. G. Ezhov, S. V. Kazin, et al., "Visual Assessment of the Influence of Adverse Diffraction Orders on the Quality of Image Formed by the Refractive-Diffractive Optical System," Komp. Opt. **38** (3), 418–424 (2014).
7. G. I. Greisukh, E. G. Ezhov, S. V. Kazin, et al., "Single-Layer Kinoforms for Cameras and Video Cameras of Mobile Communication Devices," Komp. Opt. **41** (2), 218–226 (2017).
8. G. I. Greisukh, E. G. Ezhov, S. V. Kazin, and S. A. Stepanov, " Effect of Side Diffraction Orders on Imaging Quality Produced by a Refractive/Diffractive Objective in a Digital Camera," Opt. Zh. **83** (3), 27–31 (2016).
9. V. A. Lukin, K. S. Mustafin, and R. A. Rafikov, "Hologram Optical Element," RF Patent 1271240, Publ. 05.10.1996.
10. A. V. Lukin, "Holographic Optical Elements," Opt. Zh. **74** (1), 80–87 (2007).
11. Y. Arieli, S. Noach, S. Ozeri, and N. Eisenberg, "Design of Diffractive Optical Elements for Multiple Wavelengths," Appl. Opt. **37** (26), 6174–6177 (1998).
12. G. I. Greisukh, E. G. Ezhov, and S. A. Stepanov, "Choosing Materials for Achromatization of Relief-Phase Diffraction Structures," Komp. Opt. **32** (1), 43–46 (2008).
13. G. I. Greisukh, E. A. Bezus, D. A. Bykov, et al., "Suppression of the Spectral Selectivity of Two-Layer Phase-Relief Diffraction Structures," Opt. Spektrosk. **106** (4), 694–699 (2009).
14. V. P. Koronkevich and I. G. Palchikova, "Modern Zone Plates," Avtometriya, No. 1, 85–100 (1992).
15. G. I. Greisukh, E. G. Ezhov, A. V. Kalashnikov, et al., "The Efficiency of Relief-Phase Diffractive Elements at a Small Number of Fresnel Zones," Opt. Spektrosk. **113** (4), 468–473 (2012).
16. G. I. Greisukh, E. G. Ezhov, Z. A. Sidyakina, and S. A. Stepanov, "Relief-Phase Diffractive Optical Elements on Revolution Surfaces Having High Diffraction Efficiency," Komp. Opt. **37** (1), 45–50 (2013).
17. T. Nakai, "Diffractive Optical Element and Optical System Having the Same," US Patent 6262846 B1, Publ. 17.07.2001.
18. Y. H. Zhao, C. J. Fan, C. F. Ying, and S. H. Liu, "The Investigation of Triple-Layer Diffraction Optical Element with Wide Field of View and High Diffraction Efficiency," Opt. Commun. **295**, 104–107 (2013).
19. Y. H. Zhao, C. J. Fan, C. F. Ying, and H. Wang, "The Investigation of Three Layers Diffraction Optical Element with Wide Field of View and High Diffraction Efficiency," Optik. **124** (20), 4142–4144 (2013).
20. T. Nakai, "Diffractive Optical Element and Optical System Having the Same," US Patent 2001/0038503, Publ. 08.11.2001.
21. B. H. Kleemann, M. Seesselberg, and J. Ruoff, "Design Concepts for Broadband High-Efficiency DOEs," J. Europ. Opt. Soc. Rapid Publ. **3**, 08015 (2008).
22. T. Gühne and J. Barth, "Strategy for Design of ASchromatic Diffractive Optical Elements with Minimized Etch Depths," Appl. Opt. **52** (34), 8419–8423 (2013).
23. C. Xue and Q. Cui, "Design of Multilayer Diffractive Optical Elements with Polychromatic Integral Diffraction Efficiency," Opt. Lett. **35** (7), 986–988 (2010).
24. G. I. Greisukh, V. A. Danilov, E. G. Ezhov, et al., "Spectral and Angular Dependences of the Efficiency of Relief-Phase Diffractive Lenses with Two- and Three-Layer Microstructures," Opt. Spektrosk. **118** (6), 118–125 (2015).
25. G. I. Greisukh, V. A. Danilov, E. G. Ezhov, et al., "Comparison of Electromagnetic and Scalar Methods for Evaluation of Efficiency of Diffractive Lenses for Wide Spectral Bandwidth," Opt. Commun. **338**, 54–57 (2015).
26. H. Yang, C. Xue, C. Li, and J. Wang, "Optimal Design of Multilayer Diffractive Optical Elements with Effective Area Method," Appl. Opt. **55** (7), 1675–1682 (2016).

27. L. Yang, Q. Cui, T. Liu, and C. Xue, "Effects of Manufacturing Errors on Diffraction Efficiency for Multilayer Diffractive Optical Elements," Appl. Opt. **50** (32), 6128–6133 (2011).
28. M. Piao, Q. Cui, H. Zhu, et al., "Diffraction Efficiency Change of Multilayer Diffractive Optics with Environmental Temperature," Journ. Opt. **16** (3), 035707 (2014).
29. G. I. Greisukh, E. G. Ezhov, S. V. Kazin, et al., "Visual Assessment of the Influence of Adverse Diffraction Orders on the Quality of Image Formed by the Refractive-Diffractive Optical System," Komp. Opt. **38** (3), 418–424 (2014).
30. G. I. Greisukh, V. A. Danilov, E. G. Ezhov, et al., "Spectral and Angular Dependences of the Efficiency of Relief-Phase Diffractive Lenses with Two- and Three-Layer Microstructures," Opt. Zh. **82** (5), 56–61 (2015).
31. G. I. Greisukh, E. G. Ezhov, and S. A. Stepanov, "Taking Diffractive Efficiency into Account in the Design of Refractive/Diffractive Optical Systems," Opt. Zh. **83** (3), 32–38 (2016).
32. T. Nakai and H. Ogawa, "Research on Multi-Layer Diffractive Optical Elements and Their Application to Camera Lenses," in *Proc. of the Conf. "Diffractive Optics and Micro-Optics"*. Tucson (USA), June 3, 2002. DMA2.
33. T. Nakai, "Diffractive Optical Element and Optical System Having the Same," US Patent 2007/0297057 A1, Publ. 27.12.2007.
34. F. Changjiang, "The Investigation of Large Field of View Eyepiece with Multilayer Diffractive Optical Element," Proc. SPIE. **9272**, 92720N-1 (2014).
35. G. I. Greisukh, E. G. Ezhov, S. V. Kazin, and S. A. Stepanov, "Layout and Design of a Periscope-Type Refraction-Diffraction Objective for a Mobile Communication Device," Opt. Zh.**83** (11), 51–57 (2016).
36. G. I. Greisukh, E. G. Ezhov, Z. A. Sidyakina, and S. A. Stepanov, "Design of Plastic Refractive-Diffractive Compact Zoom Lenses for Visible-Near-IR Spectrum," Appl. Opt. **52** (23), 5843–5850 (2013).
37. V. G. Pospekhov and A. V. Kryukov, "Study and Calculation of Compact Periodic-Type Zoom Lens," Inzhen. Zh. Nauka Innov. **7** (2013). http://engjournal.ru/catalog/ pribor/optica/826.html.